VU VRIJE UNIVERSITEIT AMSTERDAM

VU Research Portal

Validation of GOME polarization measurements by method of limiting atmospheres

Krijger, J.M.; Tanzi, C.P.; Aben, I.; Paul, F.

published in
Journal of Geophysical Research. Atmospheres
2005

DOI (link to publisher)
10.1029/2004JD005184

document version
Publisher's PDF, also known as Version of record

Link to publication in VU Research Portal

citation for published version (APA)
Krijger, J. M., Tanzi, C. P., Aben, I., & Paul, F. (2005). Validation of GOME polarization measurements by method of limiting atmospheres. *Journal of Geophysical Research. Atmospheres*, *110*(D7). https://doi.org/10.1029/2004JD005184

General rights
Copyright and moral rights for the publications made accessible in the public portal are retained by the authors and/or other copyright owners and it is a condition of accessing publications that users recognise and abide by the legal requirements associated with these rights.

- Users may download and print one copy of any publication from the public portal for the purpose of private study or research.
- You may not further distribute the material or use it for any profit-making activity or commercial gain
- You may freely distribute the URL identifying the publication in the public portal ?

Take down policy
If you believe that this document breaches copyright please contact us providing details, and we will remove access to the work immediately and investigate your claim.

E-mail address:
vuresearchportal.ub@vu.nl

Download date: 04. May. 2023

Validation of GOME polarization measurements by method of limiting atmospheres

J. M. Krijger, C. P. Tanzi, I. Aben, and F. Paul
SRON National Institute for Space Research, Utrecht, Netherlands

Received 1 July 2004; revised 22 December 2004; accepted 10 January 2005; published 7 April 2005.

[1] A method is presented for validation of space-based polarization measurements. The method is based on a determination of limits in the (fractional) polarization of reflected solar light as measured by the GOME instrument. These empirical limits were used to study the instrument performance during the first 5.5 years of GOME operation (1996–2001), which revealed a wavelength and viewing angle-dependent degradation of the GOME polarization measurement devices. Degradation correction factors are derived under the assumption that these polarization limits remain constant in time. Using results from earlier GOME studies on clouds, Lambertian equivalent reflectance, and geolocations, it is shown that these limits correspond to cloud-free scenes with minimal aerosol load and minimal surface albedo in the case of highly polarized observations, or to clouded scenes in the case of unpolarized observations. The polarization state of the atmosphere corresponding to observations of extremely highly polarized scenes is verified using vector radiative transfer calculations.

Citation: Krijger, J. M., C. P. Tanzi, I. Aben, and F. Paul (2005), Validation of GOME polarization measurements by method of limiting atmospheres, *J. Geophys. Res.*, *110*, D07305, doi:10.1029/2004JD005184.

1. Introduction

[2] Satellite-based passive remote sensing is commonly used to derive global information about the composition of the Earth's atmosphere. Information about the total column or even vertical profiles of different gases in the Earth atmosphere can be obtained by measuring the radiance (intensity) spectrum of sunlight reflected by the Earth's atmosphere, since these spectra contain absorption bands of gases present in the atmosphere, such as ozone. The Global Ozone Monitoring Experiment (GOME) is an example of an operational space-based spectrometer that measures the radiance of reflected sunlight in the ultraviolet, visible and near-infrared wavelength range (240–800 nm) with modest spectral resolution (0.2–0.4 nm) [*Burrows et al.*, 1999]. GOME is on ESA's second European Remote Sensing satellite (ERS-2) which was launched on 21 April 1995.

[3] Although direct, unscattered sunlight is unpolarized, the sunlight reflected in the Earth's atmosphere and by the surface is generally polarized mostly because of scattering by atmospheric gaseous molecules and aerosol particles. Studies such as those by *Mishchenko and Travis* [1997]; *Herman et al.* [1997]; *Stam et al.* [1999]; *Chowdhary et al.* [2001]; *Hasekamp and Landgraf* [2002] have shown that the degree of polarization of reflected sunlight contains information on the atmospheric composition. However, for an instrument such as GOME, which aims at measuring the radiance of reflected sunlight, the polarization of this light is considered a nuisance. GOME, but also some of its successors such as SCIAMACHY on ENVISAT (launched in 2002) and GOME-2 on EUMETSAT's Metop series (planned launches 2005, 2010, and 2015), are highly polarization-sensitive instruments due to the instrument's gratings and mirrors. Neglect of such an instrument's polarization sensitivity can lead to errors in the radiances of several tens of percents at wavelengths where the instrument polarization sensitivity is highest. In order to account for this polarization sensitivity, GOME measures the polarization of reflected sunlight using three broadband detectors, the so-called polarization measurement devices (PMDs).

[4] So far only a few methods have been developed to validate GOME polarization measurements. One method relies on the identification of specific locations along the orbit at which the scattering geometries are such that the intensities of the parallel and orthogonal polarization components of the light are equal regardless of the atmosphere and surface [*Aben et al.*, 2003]. Another method relies on the identification of backscattering geometries for which the reflected light is expected to be unpolarized (N. Schutgens, private communication, 2004). These are very special cases and there is a need for a more robust and general validation method that can be applied across the full range of expected polarization values. In this paper we present such a validation method, which is applicable to the full range of GOME polarization values.

[5] The method is based on the identification of limits in the polarization values for different viewing geometries which appear to be stable in time. We show that these extremely high and low polarization cases correlate with

Copyright 2005 by the American Geophysical Union.
0148-0227/05/2004JD005184$09.00

Table 1. Spectral Ranges of the GOME Main Spectrometer and PMDs

Channel/PMD	Range, nm	Effective Wavelength, nm
Channel 1	237–315	
Channel 2	312–406	
Channel 3	397–609	
Channel 4	576–794	
PMD 1	295–397	355
PMD 2	397–580	485
PMD 3	580–745	700

certain atmospheric conditions by using GOME information on clouds [*Koelemeijer et al.*, 2001, 2002] and Lambertian equivalent reflectivity [*Koelemeijer et al.*, 2003] as well as the actual geolocation of the observation. The highly polarized GOME measurements correspond to observations of cloud-free scenes with minimal aerosol load and minimal surface albedo, while the extremely low polarized GOME observations correspond to fully clouded observations. We studied the evolution in time (1996–2001) of the polarization limits for the GOME polarization measurements in the three different wavelength bands. This showed that the limits in observed polarization are indeed constant in time except where there is observable degradation in one or more of the PMDs. The obtained limits are then used to quantify this degradation for the three PMDs as a function of viewing direction. The limits in the measured GOME polarization were verified with vector radiative transfer calculations for the case of the highly polarized observations. For the case of the lowly polarized observations the limits correspond to cloudy observations and the location of the limits is validated with cloud fraction measurements.

[6] The structure of this paper is as follows. In section 2 we describe the polarization characteristics of reflected sunlight. The GOME polarization measurements are presented and analyzed in section 3. In section 4 we present the evolution in time of the observed limits in GOME polarization and focus on instrument performance degradation. In section 5, GOME information on clouds and Lambertian equivalent reflectivity as well as the actual geolocation of the observation are used to correlate the observed limits in polarization with specific atmospheric conditions. The verification using a vector radiative transfer model is presented in section 6. We finish with conclusions in section 7.

2. Polarization Measurements and Correction

2.1. GOME Observations

[7] GOME is a spectrometer, in which light arriving from the Sun-illuminated atmosphere is dispersed and measured by four individual channels, covering the spectral range 240–790 nm (see Table 1). The light is measured in each spectral channel with a 1024-element Si-diode array.

[8] In addition to the four spectral channels in the main spectrometer, three broadband PMDs are used to measure a fixed fraction of the parallel polarized incoming light corresponding roughly to channels 2, 3 and 4 (see Table 1). The PMD effective wavelength is determined from the central wavelength of their respective sensitivity range.

[9] GOME is a nadir-viewing instrument which uses a scan mirror to sweep the instantaneous field of view of $2.9^\circ \times 0.14^\circ$ (along x across rack) over the Earth surface. During nominal operations such a forward sweep is performed in 4.5 s after which the mirror is moved back quickly in 1.5 s, in order to begin the next forward sweep. The maximum viewing nadir angle during nominal operations is about 20°. The entire sweep is split in four observations consisting of measurements of 1.5 s, referred to hereafter as the east, nadir, west and back scans. The east, nadir and west scans each have a rectangular footprint on the Earth surface of about 40 km × 320 km or $0.36^\circ \times 2.9^\circ$ (along x across track), while the back scan has a footprint of 40 km × 960 km or $0.36^\circ \times 8.7^\circ$.

[10] The GOME PMDs are read out every 93.74 ms. The signal is then coadded (16 readouts) to an effective integration time of 1.5 s in the on-ground data processing corresponding with the integration time of the signal in the main channels. The PMDs in conjunction with the main channel spectral data are then used to correct for the GOME polarization sensitivity.

2.2. GOME Polarization

[11] Although direct, unscattered sunlight is unpolarized, sunlight reflected by the Earth's atmosphere is generally polarized because of scattering by atmospheric gaseous molecules and aerosol particles. Note that the amount of circularly polarized light reflected by the Earth's atmosphere is negligible [*Coulson*, 1988], and therefore only linearly polarized light is considered here. The polarization of the incoming light is determined by combining the broadband PMD measurements with the corresponding integrated main channel signals. The polarization sensitivity of both measurements is known from the on-ground calibration. Both measurements thus measure a known fraction of the (linearly polarized) incoming light. By combining the information from these measurements, the fractional polarization can be obtained. The GOME fractional polarization p is the polarization quantity which is relevant in the GOME polarization correction algorithm. Equation (1) shows the expression that is used in the GOME data processor to derive the GOME fractional polarization p:

$$S_{\mathrm{PMD}} = \sum_i p\,\xi_i \frac{S_i}{p(1-\eta_i)+\eta_i}. \qquad (1)$$

S_{PMD} is the signal measured by a PMD, S_i is the signal measured by each detector pixel i (i.e. wavelengths) in the main channel, η_i is the polarization sensitivity ratio of detector pixel i, ξ_i is the ratio of the sensitivity to parallel polarized light of the PMD with respect to each corresponding detector pixel i, and p is the GOME fractional polarization. The sum is over all main channel detector pixels (i.e., wavelengths) for which the corresponding PMD is sensitive. η_i and ξ_i have been determined on ground through calibration of the instrument. In this approach the fractional polarization is assumed constant across each PMD wavelength [*Balzer*, 1994]. The value of p for each PMD is determined from the numerical solution of equation (1) and given in the GOME data product. An additional value of p for the lower UV range below 300 nm, which is not covered by the PMDs, is derived analytically

from the Rayleigh single-scattering value [*Stammes et al.*, 1997]. These values are then used to correct the polarized signal for the polarization sensitivity of the instrument as follows:

$$C = \frac{1}{2}\frac{1+\eta}{p(1-\eta)+\eta}. \quad (2)$$

An interpolation between these four values of p yields the continuous correction factor function C across the entire wavelength range of GOME. Degradation of the GOME PMD 1 measurement has been observed and therefor an updated expression for equation (1) is used in the GOME data processor [*Tanzi et al.*, 1999; *Hegels and Slijkhuis*, 1999; *Balzer*, 1994]:

$$(1-2pD)S_{\mathrm{PMD}} = \sum_i p\xi_i \frac{S_i}{p(1-\eta_i)+\eta_i}, \quad (3)$$

with D an empirical correction factor which accounts for stray light in the PMD measurements, and other effects, like the observed PMD 1 degradation, which are not properly calibrated. The value of D is determined on a daily basis from the GOME daily extraterrestrial solar observations for which the light is known to be unpolarized.

[12] Linearly polarized light can be described by the Stokes parameters I, Q and U [*Hansen and Travis*, 1974]. The radiance I is defined independent of any reference plane, but the linear polarization parameters Q and U must be defined relative to a reference plane. For GOME this is the local meridian plane, i.e., the plane containing the local zenith and the viewing direction. Stokes parameters and all quantities derived from them are dependent on wavelength; this is assumed throughout this section in the formulae below. The degree of linear polarization P is defined by:

$$P = \frac{\sqrt{Q^2+U^2}}{I} \quad (4)$$

and the direction of polarization relative to the reference plane by:

$$\tan 2\chi = \frac{U}{Q}. \quad (5)$$

The degree of linear polarization P(λ) is a quantity which can vary between fully polarized ($P = 1$) and fully depolarized ($P = 0$) depending on wavelength and scene [*Aben et al.*, 1999; *Schutgens and Stammes*, 2002]. For GOME polarization correction it is sufficient to determine the parameter p of the incoming light and not the degree of linear polarization P, as the GOME instrument is sensitive only to light polarized parallel and orthogonal to the entrance slit, in other words, GOME is insensitive to the Stokes parameter U. Using these definitions the GOME fractional polarization p can be rewritten as follows:

$$p = \frac{1}{2}\left(1 - \frac{Q}{I}\right), \quad (6)$$

$$p = \frac{1}{2}(1 - P\cos 2\chi) \quad (7)$$

[13] In the case of unpolarized light, or polarized light with the direction of polarization $\chi = 45°$ or $135°$, p equals 0.5.

[14] A more physically meaningful parameter than the GOME fractional polarization p is the fractional polarization parameter $q(= Q/I)$, as this relates directly to the Stokes parameter. The fractional polarization parameter q is related to p through $q = 1 - 2p$. In the rest of this study we use q instead of p.

3. Polarization Observations

[15] For this study we use GOME polarization observations performed from the start of GOME routine operation, March 1996, until August 2001. Only GOME observations in nominal operation, corresponding to the 960 km swath width, are used. In other words, all special observations modes like polar and narrow swath width have been skipped in the current analysis. Also all back scan measurements have been skipped. The PMD data used is already been corrected for degradation to some degree, based on solar measurements according to equation (3).

[16] The fractional polarization in Earth-reflected radiation is limited by the Rayleigh single-scattering value (q_{ss}), appropriate to the viewing geometry [*Aben et al.*, 1999]. Measured fractional polarization must, in absolute value, be smaller than or equal to the absolute value of the Rayleigh single-scattering value (except in special cases such as sunglint and rainbows), yet must retain the same sign, as the atmosphere only depolarizes the light through multiple scattering, and at maximum completely depolarize the light ($q = 0$). This is graphically shown in Figure 1, where the $q = 0$ and the $q = q_{\mathrm{ss}}$ lines divide the q,q_{ss} plane in 4 quadrants, with the lower left and the upper right representing the physically meaningful values ($0 \leq |q| \leq |q_{\mathrm{ss}}|$). Plotting the GOME-measured fractional polarization q as a function of q_{ss} quickly shows which measurements are unphysical as they either show stronger polarization than q_{ss} or are of opposite sign to q_{ss}.

[17] Figure 2 shows all GOME east polarization measurements q for PMD 1 for the months of March and September from March 1996 until March 2000. Most measurements indeed appear to lie largely in the two "physical" quadrants. Values near $q = q_{\mathrm{ss}} = 0$ which fall into the other quadrants can be explained by noisy measurements affecting the obtained q values.

[18] The distributions clearly show pronounced limits in the measured polarization q. The highly polarized observations are well below their corresponding q_{ss} values, whereas the observations with the lowest polarization more or less coincide with $q = 0$.

4. PMD Performance in Time

[19] In this section we monitor the PMD performance in time during the first five years of routine GOME operation. For GOME an entire month yields enough ($\sim 10^5$) measurements to statistically detect the limits in polarization, as discussed in section 3 and shown in Figure 2. Shorter periods yield too few measurements to determine the limit at the more extreme q_{ss} values, while longer periods would reduce our temporal sampling. Therefore both the extreme

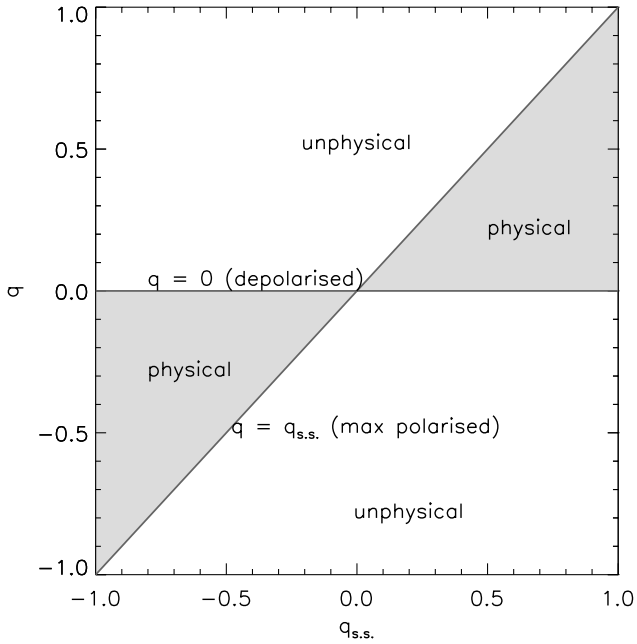

Figure 1. The range of possible (measured) q as a function of their theoretical single-scattering value q_{ss}. Shaded areas correspond to physically meaningful q values, namely q between 0 and q_{ss}.

polarization cases and the unpolarized cases may be determined for each month starting in March 1996 until August 2001 using only normal swath data in that period, excluding special pole-viewing and narrow swath modes. Several months had highly noisy polarization measurements for hardware-specific reasons (gyroscope failure and bit flips) and were not used. The limits were determined separately for each PMD (PMD 1, PMD 2 and PMD 3) and for each viewing direction (east, nadir and west) as follows: First the measurements were collected in bins of 0.05 in q_{ss} and the three most extreme values were removed as outliers. From the remaining binned measurements the most extreme values were taken as the limiting value at that particular q_{ss}. The results are shown in Figure 3.

[20] The first thing to note is that the range of q_{ss} is dictated by the range of possible scattering geometries which depends on viewing direction (east, nadir, west). Also seasonal variation of the q_{ss} range is present, corresponding to the variation in the position of the Sun. Furthermore, it is also clear from Figure 3 that the number of measurements is not always sufficient for higher q_{ss} values to establish a clear limit resulting in noise in these plots. Nonetheless, the shape of the monthly limit curves for each PMD and for each viewing direction is constant in time (except near high q values where the number of observations is low). Also, the actual position of the curves is rather

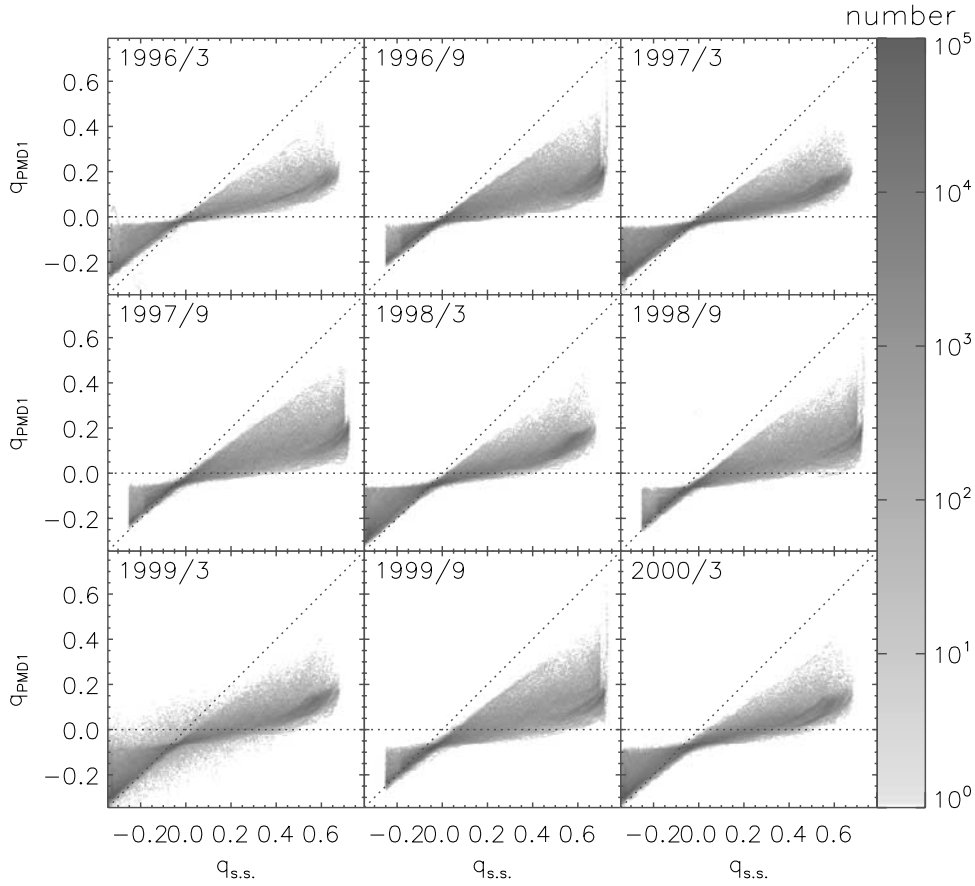

Figure 2. The number of measured fractional polarization values q (PMD 1 east pixels only) as a function of q_{ss} per 0.05 q,q_{ss} width bins for several months of GOME observations (the month is indicated in the upper left corner of each panel). Note that March 1999 shows more noisy behavior owing to hardware problems (gyroscope and bit flips). See color version of this figure in the HTML.

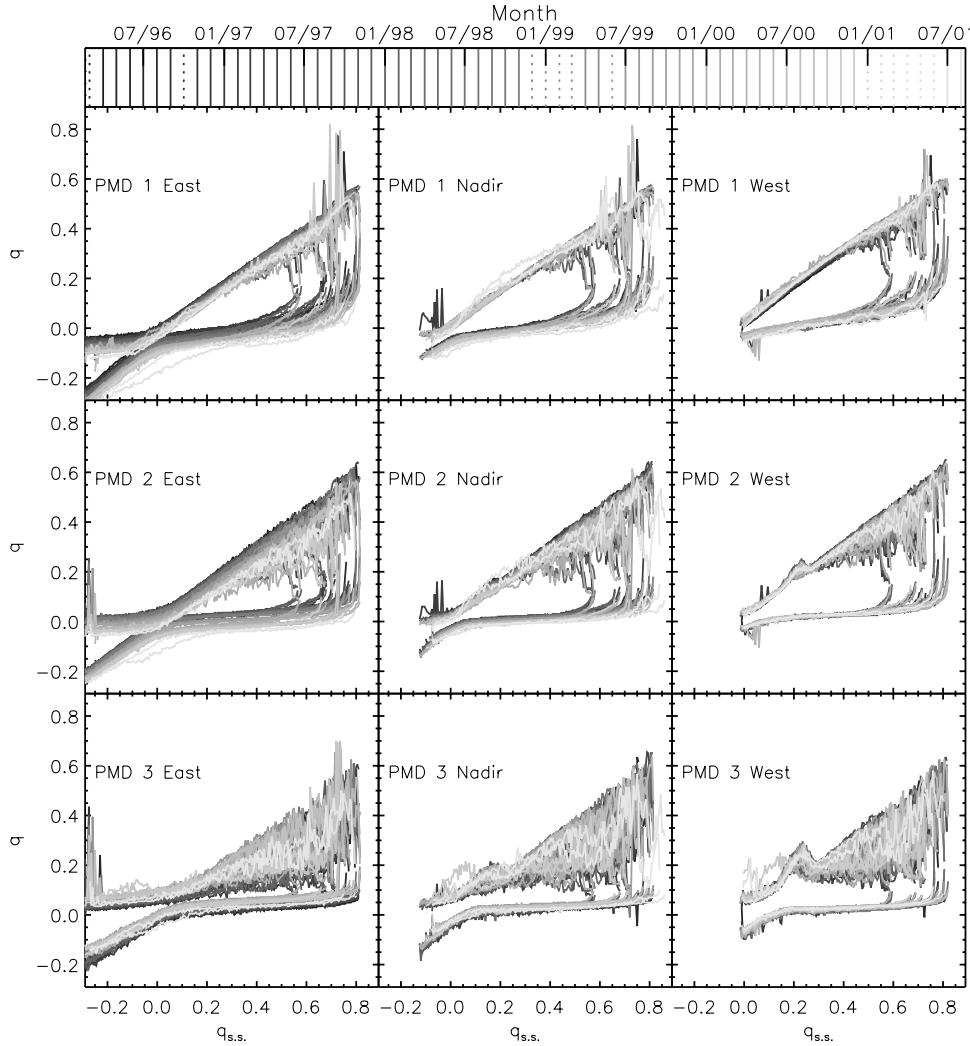

Figure 3. Measured limits in q for all PMDs and viewing directions for each month of GOME polarization measurements, excluding back scans, narrow swath, and polar views. Each month is color-coded as indicated at the top of the plot. Several months (e.g., around January 1999 and March 2001) are not shown, indicated by a dashed colored line at the top of the plot, because during those months GOME suffered from hardware problems (gyroscope and bit flips). See color version of this figure in the HTML.

constant except in some cases, most notably for the PMD 2 east observations, where a shift of the curves in time is evident. We attribute these shifts in observed polarization limits to degradation in instrument performance.

[21] It is possible to quantify the change in time in observed limits with a simple time-dependent offset relative to April 1996. These offsets are determined for each month and shown in Figure 4. Offsets obtained both by the extremely polarized limit, the nearly unpolarized limit and the so-called $p = 0.5$ method [*Aben et al.*, 2003] are shown. All three methods are in very good agreement with one another.

[22] A second-degree polynomial in time is fitted to the limits obtained from the unpolarized measurements (the limit of extremely polarized measurements suffer from sparse data for some months). The fit results are shown as well in Figure 4 and tabulated in Table 2 along with their uncertainties (1σ). The obtained behavior of the offsets can be used to correct for the instrument degradation.

[23] Figure 4 shows that the instrument degradation observed is most severe for the east direction, much less for the nadir direction and the least for the west direction. PMD 1 and PMD 2 in east direction clearly suffer the most from degraded performance. The different behavior for the different viewing geometry points to a scan angle-dependent component in the degradation.

5. Identification of the Limiting Atmosphere

5.1. Introduction

[24] Unpolarized light from the Sun becomes polarized in the Earth's atmosphere. The general behavior of the fractional polarization along the orbit is mainly determined by molecular scattering (Rayleigh scattering), while local variability of q is due to the presence of clouds and/or aerosols and changes in surface albedo [*Stammes et al.*, 1997]. The degree of linear polarization from Rayleigh single scattering q_{ss} is only valid for UV wavelengths (below 300 nm), where

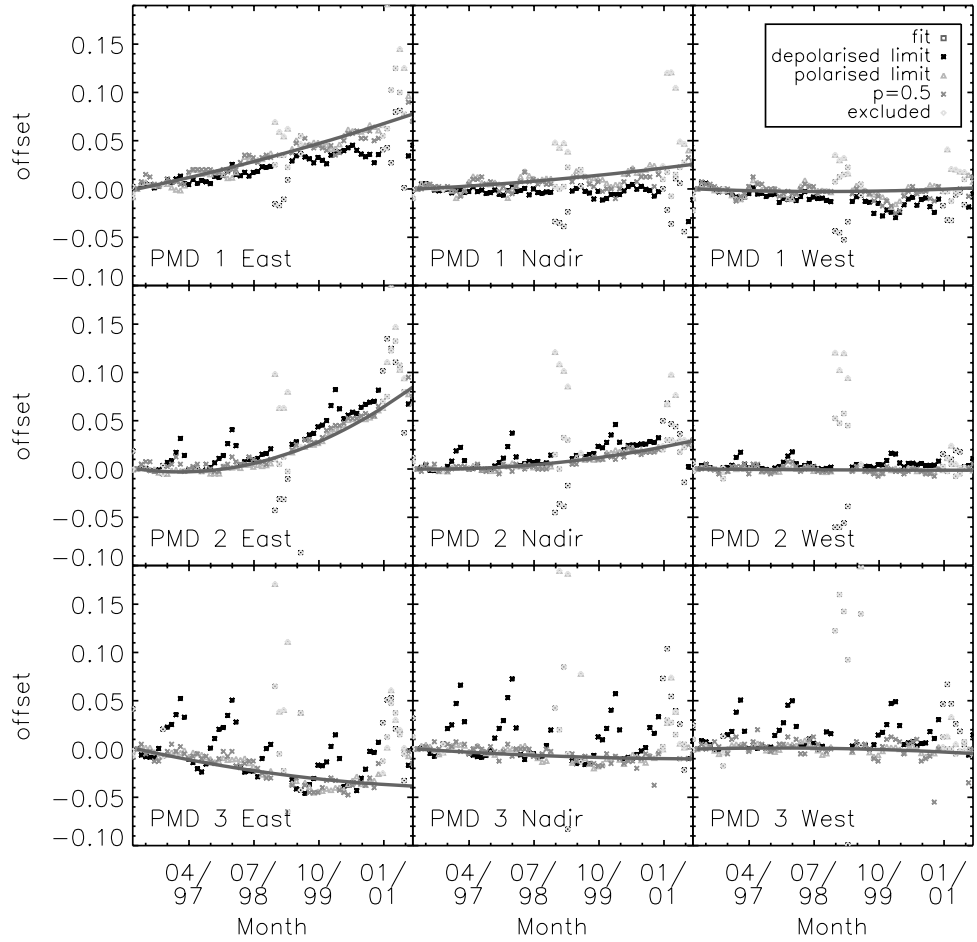

Figure 4. Measured offsets for all PMDs and viewing directions over 5.5 years of GOME polarization measurements. Offsets determined from the extreme polarization limit are shown in black, while those for the nearly unpolarized limit are shown in blue. The offset determined from the so-called $p = 0.5$ method [*Aben et al.*, 2003] is shown in cyan. The extreme polarization limit offsets suffer from statistical limitations in certain months of the year, which explains the systematic yearly deviation of some of the high polarization limits (black). In addition, several months (in red) were excluded because of satellite hardware problems (gyroscope and bit flips). The second-degree polynomial fit (Table 2) has been shown as a continuous green curve. See color version of this figure in the HTML.

single scattering dominates because of the very strong ozone absorption. At longer wavelengths, multiple scattering by aerosols becomes more dominant, which depolarizes the light.

[25] Furthermore clouds cause enhanced multiple scattering, and because light reflected at the Earth's surface is in most cases strongly depolarized, we expect the most extremely polarized observations to occur for atmospheres with minimal aerosol load over cloud-free scenes with minimal surface albedo. We will verify this assumption in the following subsections, using the available cloud fractions and reflectance values corresponding to each individual GOME measurement [*Koelemeijer et al.*, 2001, 2002, 2003].

5.2. Polarization Limits and Correlation With Clouds

[26] GOME reflectance measurements in and around the O_2 A band have been used by *Koelemeijer et al.* [2002] to derive effective cloud fractions for each individual GOME measurement. Cloud fractions range between 0 and 1 which corresponds to no clouds and fully clouded observations, respectively. The absolute uncertainty for all these cloud fractions is 0.1. In Figure 5 the east July 1996 observations for the three different PMD measurements are shown. The

Table 2. Second-Degree Fit Parameters With Their 1σ Uncertainty Corresponding to the Polynomial Fit Shown in Figure 4[a]

	P_1, 10^{-5}	(1σ), 10^{-5}	P_2, 10^{-8}	(1σ), 10^{-8}
PMD 1 east	3.05	(0.23)	0.48	(0.17)
PMD 1 nadir	0.73	(0.26)	0.30	(0.18)
PMD 1 west	−0.59	(0.29)	0.33	(0.20)
PMD 2 east	−1.98	(0.18)	3.25	(0.13)
PMD 2 nadir	−0.19	(0.18)	0.87	(0.12)
PMD 2 west	−0.12	(0.20)	0.03	(0.13)
PMD 3 east	−3.27	(0.21)	0.67	(0.15)
PMD 3 nadir	−0.99	(0.19)	0.24	(0.13)
PMD 3 west	0.35	(0.19)	−0.30	(0.13)

[a]The parameters are given as a function of numbers of days since 1 April 1996 (day): $P_1 \times \text{day} + P_2 \times \text{day}^2$.

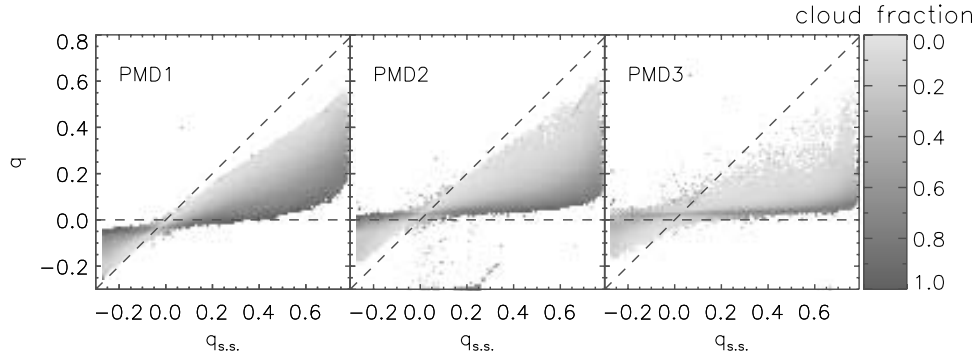

Figure 5. Measured fractional polarization values as a function of their theoretical single scattering value (for PMD 1, 2, and 3 separately), east pixels only during July 1996. Each measurement is color-coded according to its cloud fraction. See color version of this figure in the HTML.

data are color-coded according to their cloud fraction. The observations in Figure 5 are representative for the GOME data set studied here, and clearly show the correlation between cloud fraction and fractional polarization q. The most extremely polarized measurements correspond to cloud-free observations and the least polarized measurements to fully clouded observations. Cloud fraction smoothly increases while moving from the most extreme polarized scenes to the unpolarized cases.

5.3. Polarization Limits and Correlation With Lambertian Equivalent Reflectance

[27] The Lambertian equivalent reflectance (LER) is the effective atmospheric reflectivity assuming a Rayleigh atmosphere above a Lambertian surface [*Koelemeijer et al.*, 2003]. The LER value is obtained first by correcting the observed GOME reflectivities for the main absorber O_3. Then the GOME reflectivities are modelled assuming a Rayleigh atmosphere bounded below by a Lambertian surface. The surface albedo is adjusted so that the modelled reflectivities correspond to the GOME reflectivities. The GOME LER values are derived at different wavelengths by *Koelemeijer et al.* [2003] and provided in a database covering 5.5 years of GOME observations.

[28] In Figure 6 the east July 1996 observations for the three different PMD measurements are shown again with the fractional polarization q plotted against the corresponding single-scattering q_{ss} value. Now only those measurements are shown that were identified as cloud-free (cloud fraction ≤ 0.1). The data is color-coded according to their LER values. The observations clearly show the correlation between LER value and fractional polarization q. The most extremely polarized measurements correspond to low LER values, the least polarized measurements correspond to high LER values. In between, the LER values increase smoothly while moving from the most extreme polarized scenes to the less polarized cases.

5.4. Polarization Limits and Their Geolocations

[29] We binned all cloud-free polarization measurements for a single month (July 1996) into q_{ss} bins of 0.001 width for all PMDs and selected in each bin 5% of the data closest to the respective q_{ss} value. The locations of these most extremely polarized measurements are shown in Figure 7 for two different GOME PMDs, color-coded with their respective LER value. The plot for PMD 2 shows little extra information and has been omitted. The observed latitudinal distribution is caused by the patterns of clouds present. The Northern Hemisphere contains far less cloud-free scenes compared to the Southern Hemisphere during the month of July. For extremely polarized PMD 1 measurements the locations are more randomly distributed over

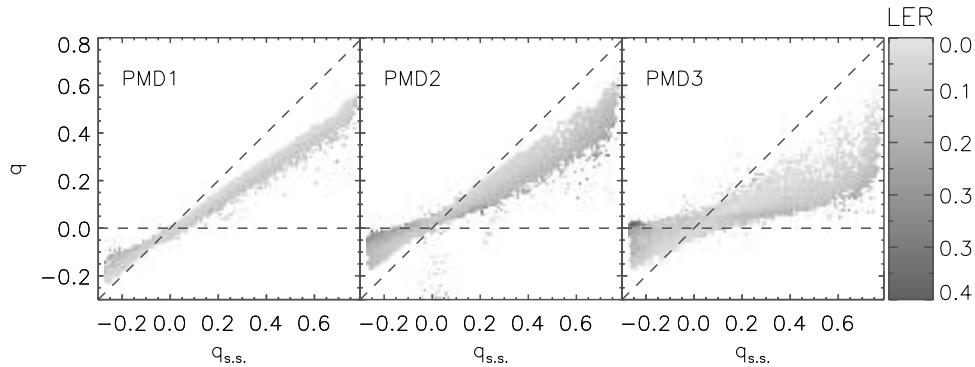

Figure 6. Measured fractional polarization values as a function of their theoretical single-scattering value (for PMD 1, 2, and 3) cloud-free (cloud fraction ≤ 0.1), east pixels only during July 1996. Each measurement is color-coded according to the LER value closest to the corresponding PMD effective wavelength (335, 494, and 670 nm for PMD 1, 2, and 3, respectively). See color version of this figure in the HTML.

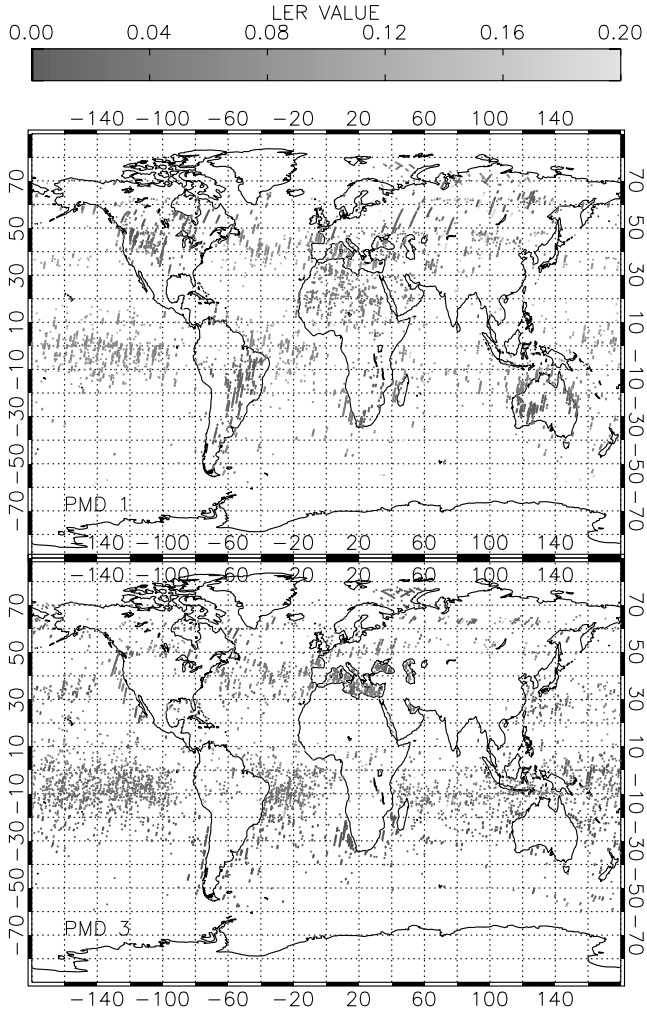

Figure 7. Locations of the relatively most (top 5%) extremely polarized measurements (cloud-free), color-coded with their corresponding LER value. Top panel PMD 1 (with LER values at 335 nm), bottom panel PMD 3 (with LER values at 670 nm) during July 1996, all viewing directions. See color version of this figure in the HTML.

longitude (over land and ocean), while for PMD 3 these measurements appear to correlate with the oceans.

[30] The difference between the geolocations of extremely polarized PMD 1 and PMD 3 observation is consistent with the notion that high surface albedo in general depolarizes the reflected sunlight. At the wavelengths covered by PMD 1 (~355 nm), the surface albedo is low, regardless of the actual surface type (ocean or land), while for the effective wavelengths of PMD 3 (~700 nm) the land has a much higher albedo than that for water. Therefore the highest polarized PMD 3 observations are seen over oceans only, whereas they occur equally over land or ocean for PMD 1.

6. Model Calculations

[31] In this section we use a vector radiative transfer code to simulate the expected polarization for atmospheric scenes corresponding to the extremely polarized GOME observations as derived in the previous sections. The calculated polarization is used to verify quantitatively the extreme polarization values obtained from the measurements. A doubling-adding code (hereinafter referred to as DAP; *Stam et al.* [2000]) is used, which calculates I(λ), Q(λ) and U(λ). Rayleigh scattering, ozone absorption and Mie scattering from aerosols are included in radiative transfer, with a 33-layer plane-parallel atmosphere bounded below by a Lambertian surface. No aerosols were included for these initial calculations. Other molecular absorption and Raman scattering processes are not included in the calculations. (This is not considered a limitation because these contribute mainly to high frequency spectral features which have little effect on the GOME PMD broadband measurements.) The atmospheric profiles (pressure, temperature and ozone density) in the calculations are representative of a midlatitude summer as the average measured by two ozone sondes on 14 and 21 August 1998 at KNMI, de Bilt. In all cases the total ozone column was 300 DU. The initial calculations were done for an atmosphere without aerosols and an assumed black (nonreflecting) ground surface. In order to simulate the GOME-measured q values the calculated I and Q values (GOME is insensitive to U polarization) were convolved according to the GOME PMD wavelength-dependent (instrument) radiance sensitivities. The calculations were performed at various illumination geometries which are representative for the most extreme polarized GOME observations. The variation of illumination geometrie over the field of view of a GOME PMD observation was ignored, as the effect is smaller then a few percent in fractional polarization value. The results are shown in Figure 8 and show that the calculated q values, for a purely molecular atmosphere, approach the theoretical Rayleigh single-scattering values as the wavelength increases (from PMD 1 to PMD 3). This is as expected because the polarization increases smoothly beyond $\lambda \sim$ 320 nm due to the wavelength dependence of the Rayleigh-scattering optical thickness. The polarization will approach its single-scattering value near the long wavelengths ($\lambda \geq$ 600 nm), without any reflection at the surface, assuming a purely molecular atmosphere.

[32] In Figure 8 the GOME east polarization measurements from July 1996 illustrate that the measured fractional polarization q is always below the value obtained by these calculations, which is as expected since the Rayleigh atmosphere is a limiting, hypothetical case with the highest degree of polarization. The presence of scatterers such as aerosols changes this calculated upper limit, yielding progressively less polarized light with increasing aerosol load and increasing surface albedo, most noticeably at the longer wavelengths [*Aben et al.*, 1999].

[33] As we are looking for the atmosphere that corresponds best with the observed limit in polarization we must include surface albedos and an aerosol load corresponding to a realistic atmosphere. Therefore we performed a number of simulations in which the surface albedo and aerosol load were varied independently. The aerosol type was fixed to oceanic origin maritime aerosols [*Shettle and Fenn*, 1979] in the calculations because in section 5.4 it was shown that the most extreme polarized observations occur over the ocean for all PMDs (low albedo at all wavelengths). The

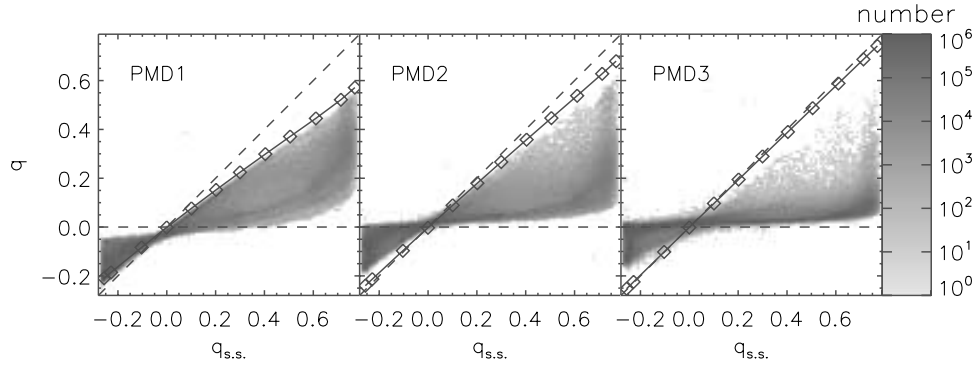

Figure 8. Limits in polarization calculated with a doubling adding code for a purely molecular atmosphere and a black surface (red squares). Calculations are performed at representative GOME illumination geometries. The measured fractional polarization values q (PMD 1 east pixels only) are shown as a function of q_{ss} per 0.05 q,q_{ss} width bins for July 1996 and are color-coded according to the number of occurrences as defined on the right-hand side. See color version of this figure in the HTML.

optical thickness of the aerosols can be increased to represent an increase in the total amount of aerosols present.

[34] Figure 9 shows the results of the calculations where only the surface albedo was varied from 0.0 to 0.02 in steps of 0.002, without any aerosols present. For comparison purposes, the figure also includes the derived, time-averaged (degradation-corrected) measured polarization limits. We conclude from a weighted least squares fit that the GOME PMD1, PMD2 and PMD3 extreme polarization limiting cases correspond roughly to atmospheres with a Lambertian equivalent reflectivity of 0.05 ± 0.05,0.02 ± 0.01, 0.012 ± 0.004, respectively. This Lambertian equivalent reflectivity includes the combined effect of surface albedo reflectivity and aerosol scattering.

[35] However aerosols have a different polarization effect than the surface reflectivity and so we also varied independently the surface albedo and the maritime aerosol optical thickness (AOT) in our simulations. With different combinations of albedo and AOT we can perform weighted least squares fits to find a reasonable combination of albedo and AOT that results in a limit that matches the observed limit. The best fits are shown in Figure 10, which summarizes our results by showing the obtained limits for all PMDs and viewing directions averaged over 5.5 years of GOME polarization measurements and the same limit according to our best fit modelled atmosphere.

[36] Note that the measured polarization limit for the east viewing direction is always lower than the limits determined in west or nadir direction for PMD 3. This might be an indication that an incorrect calibration or already a instrument scan angle-dependent degradation had taken place for the measurements obtained during April 1996 (our reference month). The measured polarization limits averaged over time for all viewing directions can be fitted with modelled atmospheres. The least squares fits have been restricted to the data corresponding to q_{ss} values between −0.2 and 0.4, to avoid under-sampling effects at the more extreme q_{ss} values. The best estimated atmosphere contains maritime aerosol with an AOT of 0.04 (at 550 nm) and surface albedo of 0.02, 0.015, 0.012 for PMD 1,2 and 3, respectively. This seems to us reasonable values for low surface albedo scenes [*Koelemeijer et al.*, 2003] and minimal aerosol load atmosphere [*Holben et al.*, 2001].

[37] The q values plotted in Figure 10 show distinct features near q_{ss} = 0.2 in the nadir and west PMD 2 and PMD 3 observations. These are caused by the scattering of light on water clouds (Mie particles) which give rise to highly polarized light. This is known as the rainbow effect [*Liou*, 1980]. The rainbow is not observed in the east viewing direction because the rainbow geometry with scattering angles of ∼140° is not present: this geometry is most often reached in the west viewing direction. The effect

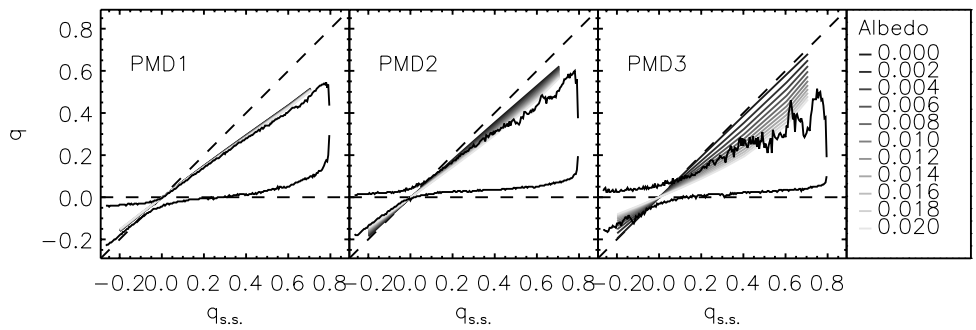

Figure 9. Limits in polarization calculated for a pure molecular atmosphere with varying surface albedo (color-coded as indicated on the right). The measured limits for July 1996 (east pixels) are indicated in black. See color version of this figure in the HTML.

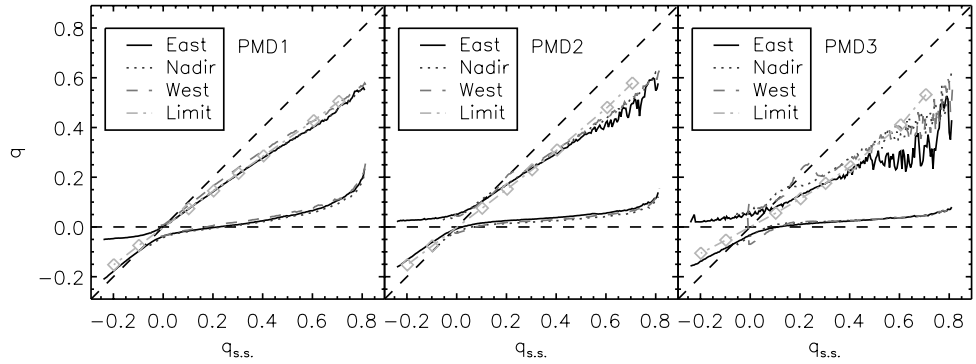

Figure 10. Polarization limits for all PMDs and viewing directions averaged over 5.5 years of GOME polarization measurements. Model calculations are also shown (cyan block and solid line) for an atmosphere with maritime aerosol with an optical thickness of 0.04 (at 550 nm) and surface albedo of 0.02, 0.015, and 0.012 at the effective wavelengths corresponding to PMD1, PMD2, and PMD3, respectively. The calculated limits show no significant differences for the different viewing geometries. See color version of this figure in the HTML.

becomes less clear toward the shorter wavelengths because of the increasing optical thickness of the atmosphere at these wavelengths and the increased amount of multiple scattering which lowers the high degree of polarization caused by the rainbow. This effect is currently not included in our modelled atmosphere as we did not include water clouds which are responsible for this effect.

7. Conclusions

[38] So far only a few methods have been developed to validate GOME polarization measurements in flight. One method relies on the identification of specific scattering geometries for which the scattered light is expected to be unpolarized. In this paper a validation method is presented which can be used to validate the full range of GOME polarization values. The method is based on an empirical determination of constant limits in the polarization of reflected solar light as measured by the GOME instrument. The observed maximum polarization limit corresponds to a cloud-free, minimal aerosol load atmosphere bounded below by a dark surface, while the limit corresponding to the most depolarized observations occur for clouded observations only. This is confirmed by independent information on the observed cloud fraction and Lambertian equivalent reflectivity from the GOME measurements. Radiative transfer calculations further show that the highest polarized observations correspond to a cloud-free atmosphere containing maritime aerosol with an optical thickness of 0.04 (at 550 nm) and surface albedos of 0.02, 0.015 and 0.012 for PMD1 (∼300–400 nm), PMD2 (∼400–580 nm) and PMD3 (∼580–750 nm), respectively.

[39] We used the concept of limits in polarization values to monitor the performance of the GOME PMDs during the first five years of routine GOME operation. This exercise showed that the limits in observed polarization are indeed constant in time when the instrument performance is stable. However, it also revealed degraded performance, most pronounced for the east directions, but also noticeable for PMD 1, and PMD 2 in nadir direction. The PMDs show no significant degradation for the west direction. The different behavior for the different viewing geometries indicates a scan angle-dependent component in the instrument degradation, which is consistent with previous findings on GOME main channel degradation [*Aben et al.*, 2000]. These results can be used to correct polarization measurements for the observed degradation in the GOME PMDs.

Notation

- λ wavelength, nm
- I Stokes parameter: Total intensity, J/cm^2/sec/sr
- Q Stokes parameter: Linear polarized light
- U Stokes parameter: 45° Linear polarized light
- P Total degree of linear polarization
- χ direction of polarization, degrees
- S_a Signal from source a, binary units
- η relative instrument polarization sensitivity
- ξ ratio polarization between PMD and spectral channel diode
- C Instrument polarization correction
- D empirical correction factor
- p GOME fractional polarization parameter
- q fractional polarization parameter
- q_{ss} theoretical single scattering Stokes fractional polarization parameter

[40] **Acknowledgments.** We would like to thank D. Stam for initial model calculations, W. Hartmann for valuable input, A. Maurellis for comments, R. van Hees for software codes, and L.G. Tilstra for many enlightening discussions. Financial support is acknowledged from ESA (GOME-2 study) and NIVR (SCIAMACHY phase E). ESA is acknowledged for providing GOME data ((c)ESA 1995–1996) processed by DFD/DLR.

References

Aben, I., F. Helderman, D. M. Stam, and P. Stammes (1999), Spectral fine-structure in the polarization of skylight, *Geophys. Res. Lett.*, *26*, 591–594.

Aben, I., M. Eisinger, E. Hegels, R. Snel, and C. P. Tanzi (2000), GDAQI final report, *Rep. TN-GDAQI-003SR/2000*, Eur. Space Ag., Paris.

Aben, I., C. Tanzi, H. Hartmann, D. Stam, and P. Stammes (2003), Validation of space-based polarization measurements by use of a single-scattering approximation, with application to the global ozone monitoring experiment, *Appl. Opt.*, *42*, 3610–3619.

Balzer, W. (1994), GOME level 0 to 1 algorithm description, *Rep. ER-TN-DLR-GO-022*, Dtsch. Zentrum für Luft- und Raumfahrt.

Burrows, J. P., A. Dehn, B. Deters, S. Himmelmann, A. Richter, S. Voigt, and J. Orphal (1999), Atmospheric remote-sensing reference data from GOME: 2, Temperature-dependent absorption cross sections of O_3 in the 231–794 nm range, *J. Quant. Spectrosc. Radiat. Transfer*, *61*, 509–517.

Chowdhary, J., B. Cairns, M. Mishchenko, and L. Travis (2001), Retrieval of aerosol properties over the ocean using multispectral and multiangle photopolarimetric measurements from the research scanning polarimeter, *Geophys. Res. Lett.*, *28*, 243–246.

Coulson, K. (1988), *Polarization and Intensity of Light in the Atmosphere*, A. Deepak, Hampton, Va.

Hansen, J. E., and L. D. Travis (1974), Light scattering in planetary atmospheres, *Space Sci. Rev.*, *16*, 527–610.

Hasekamp, O., and J. Landgraf (2002), A linearized vector radiative transfer model for atmospheric trace gas retrieval, *J. Quant. Spectrosc. Radiat. Transfer*, *75*, 221–238.

Hegels, H., and S. Slijkhuis (1999), GOME: Correction of degradation and update of keydata, *Rep. ESAMS, ESA WPP-161*, pp. 695–700, Eur. Space Res. and Technol. Cent., Noordwijk, Netherlands.

Herman, M., J. L. Deuzé, C. Devaux, P. Goloub, F. M. Bréon, and D. Tanré (1997), Remote sensing of aerosols over land surfaces including polarization measurements: Application to POLDER Measurements, *J. Geophys. Res.*, *102*, 17,039–17,049.

Holben, B. N., et al. (2001), An emerging ground-based aerosol climatology: Aerosol optical depth from AERONET, *J. Geophys. Res.*, *106*(D11), 12,067–12,098.

Koelemeijer, R. B. A., P. Stammes, J. W. Hovenier, and J. F. de Haan (2001), A fast method for retrieval of cloud parameters using oxygen A-band measurements from the Global Ozone Monitoring Experiment, *J. Geophys. Res.*, *106*, 3475–3490.

Koelemeijer, R. B. A., P. Stammes, J. W. Hovenier, and J. F. de Haan (2002), Global distributions of effective cloud fraction and cloud top pressure derived from oxygen A band spectra measured by the Global Ozone Monitoring Experiment: Comparison to ISCCP data, *J. Geophys. Res.*, *107*(D12), 4151, doi:10.1029/2001JD000840.

Koelemeijer, R. B. A., J. F. de Haan, and P. Stammes (2003), A database of spectral surface reflectivity in the range 335–772 nm derived from 5.5 years of GOME observations, *J. Geophys. Res.*, *108*(D2), 4070, doi:10.1029/2002JD002429.

Liou, K. N. (1980), *An Introduction to Atmospheric Radiation*, Elsevier, New York.

Mishchenko, M. I., and L. D. Travis (1997), Satellite retrieval of aerosol properties over the ocean using polarization as well as intensity of reflected sunlight, *J. Geophys. Res.*, *102*, 16,989–17,013.

Schutgens, N., and P. Stammes (2002), Parameterisation of Earth's polarisation spectrum from 290–330 nm, *J. Quant. Spectrosc. Radiat. Transfer*, *75*, 239–255.

Shettle, E. P., and R. W. Fenn (1979), Models for aerosols of the lower atmosphere and the effects of the humidity variations on their optical properties, *Environ. Res. Pap. 676 AFGL-TR-79-0214*, Air Force Geophys. Lab. (OP), Hanscom, Mass.

Stam, D., J. F. de Haan, J. W. Hovenier, and P. Stammes (1999), Degree of linear polarization of light emerging from the cloudless atmosphere in the oxygen A band, *J. Geophys. Res.*, *104*, 16,843–16,858.

Stam, D. M., J. F. De Haan, J. W. Hovenier, and P. Stammes (2000), A fast method for simulating observations of polarized light emerging from the atmosphere applied to the oxygen A-band, *J. Quant. Spectrosc. Radiat. Transfer*, *64*, 131–149.

Stammes, P., I. Aben, R. B. A. Koelemeijer, S. Slijkhuis, and D. Stam (1997), Gome polarisation validation study, in *Proceedings GOME Geophysical Validation Campaign*, vol. 414, pp. 669–674, Eur. Space Ag., Paris.

Tanzi, C., E. Hegels, I. Aben, K. Bramstedt, and A. P. H. Goede (1999), Performance degradation of GOME polarization monitoring, *Adv. Space Res.*, *23*, 1393–1396.

I. Aben, J. M. Krijger, F. Paul, and C. P. Tanzi, SRON, National Institute for Space Research, Sorbonnelaan 2, N-3584 CA Utrecht, Netherlands. (krijger@sron.nl)